Journal of Photochemistry, 4 (1975) 407 - 417

NUMERICAL STUDIES OF THE GROWTH AND DECAY OF RESONANCE FLUORESCENCE IN THE PRESENCE OF QUENCHING AND RADIATION TRAPPING

L. F. PHILLIPS*

Physical Chemistry Laboratory, University of Oxford, Oxford, OX1 3QZ (Gt. Britain)

(Received July 1, 1975)

Summary

The differential equation governing radiation trapping has been integrated numerically for a system with cylindrical symmetry and pulsed excitation. Calculated trapping times at large optical depths are in satisfactory agreement with experimentally measured values. When quenching is included the trapping times T derived from the phase-shift of the fundamental component of the fluorescence obey a Stern–Volmer equation of the form $T_0/T = 1 + k\ T_0[Q]$. The analogous Stern–Volmer equation for I_0/I, where I is either the steady-state intensity or the amplitude of the fundamental component of the fluorescence, is also quite well obeyed.

Introduction and Theory

In a previous communication [1] some useful qualitative conclusions were drawn from numerical studies of the quenching and trapping of resonance radiation in systems of very large optical depth, with a modulated exciting beam. Interest was centred on the effect of quenching on the phase shift between the fundamental components of the exciting beam and the fluorescence. The present paper describes the results of improved numerical calculations of the same type; the calculations have now progressed to the point at which significant quantitative comparisons can be made with experimental data.

The basic differential equation to be solved is [2 - 5]:

$$\frac{\partial U(r)}{\partial t} = I_{abs}(r) - [A + Q]\,U(r) + \int A.U(r')G(r', r)\mathrm{d}r' \qquad (1)$$

where $U(r)$ is the concentration of excited species at the point defined by the vector r, $I_{abs}(r)$ is the rate at which photons are absorbed from the exciting beam at r, A is the Einstein coefficient for spontaneous emission of reso-

* On leave from the University of Canterbury, Christchurch (New Zealand).

nance fluorescence (other forms of radiative deactivation being assumed absent), Q is the pseudo-first order rate constant for the quenching reaction, and $G(r', r)$ is the probability that a photon emitted at r' will be absorbed at r. The integration extends over all space. In addition to absorbing radiation which has been emitted at r', atoms at r will also emit radiation which is subsequently absorbed at r'. Provided the concentration of ground state atoms is the same at r and r', *i.e.* both points are inside the fluorescence cell, $G(r', r)$ is symmetrical, and the *net* rate of internal radiative transfer from all points r' to r is:

$$A\int [U(r') - U(r)]\ G(r', r)\mathrm{d}r' \tag{2}$$

where the integration is now limited to the volume of the cell. For points outside the fluorescence cell transfer can be assumed to be entirely one-way, and the remainder of the $-A.U(r)$ term of eqn. (1) can be set equal to:

$$-A\ T_1(r)U(r) \tag{3}$$

where the loss term $T_1(r)$ is the probability that a photon emitted at r will escape from the cell. Equation (1) can now be written:

$$\frac{\partial U(r)}{\partial t} = I_{abs}(r) - [Q + A.T_1(r)]\,U(r) + A\int [U(r') - U(r)]\,G(r', r)\mathrm{d}r' \tag{4}$$

When this equation is changed into a form suitable for numerical solution the result is:

$$\frac{\partial U_{KL}}{\partial t} = I_{KL} - [Q + T_{KL}]\,U_{KL} + \sum_{MN} [U_{MN} - U_{KL}]\,G_{KLMN} \tag{5}$$

where

$$G_{KLMN} = A\ G(r_{av})\,R_{KLMN}\Theta_{KLMN}/4\pi \tag{6}$$

Here indices K and L are used to label the volume element to which U, I and T (which now incorporates the factor A) apply, and G_{KLMN} is the rate coefficient for radiative transfer from volume MN to a point in volume KL. $G(r_{av})$ is the probability that a photon emitted in volume element MN is absorbed in a unit length of element KL; elements KL and MN are an average distance r_{av} apart. Of the other quantities in eqn. (6) R_{KLMN} is the average thickness of element MN along a line drawn from the element KL, and Θ_{KLMN} is the solid angle subtended by the element MN from a point on element KL. In order to restrict the array G_{KLMN} to four dimensions rather than six, we consider the case of a cylindrical fluorescence cell with an axial exciting beam. Each volume element, except for the central elements which are cylindrical, is then an annulus specified by a radial coordinate x and an axial coordinate z. Within an element U is constant. The best arrangement for approximating to a smooth spatial distribution of U is one in which the annuli are smallest where the gradient of U is largest. At present the annuli

decrease in size towards the cell end windows and side walls. In most of the calculations the cell has been divided by ten radially and fifteen axially, giving a total of one hundred and fifty elementary volumes. In a cell of diameter 3.0 cm and length 3.5 cm the smallest element had radial thickness 0.0200 cm and depth 0.0158 cm, while the largest was a cylindrical "core" element of radius 0.200 cm and depth 0.41 cm.

Integrating eqn. (6) from t to $t + \Delta t$, with the internal transfer rate $\sum_{MN} [U_{MN} - U_{KL}] G_{KLMN}$ held constant, gives:

$$\Delta U_{KL} = U_{KL}(t + \Delta t) - U_{KL}(t) = \{[I_{KL} + \sum_{MN} (U_{KL} - U_{MN}) G_{KLMN}] / [T_{KL} + Q] - U_{KL}(t)\}\{1 - \exp(-[T_{KL} + Q]\Delta t)\} \quad (7)$$

Using eqn. (7), the time evolution of U_{KL} can be followed from $t = 0$ until the steady state is reached, after which U_{KL} remains constant until some predetermined time at which all I_{KL} are set equal to zero and the concentration of excited species begins to decay. In this way the response of the system to a square-wave excitation pulse is simulated. The output fluorescence intensity along a radius specified by parameter L is calculated from the equation:

$$I_{out}(L) = \sum_{K} (T'_K + T''_K) U_{KL} g_{xK} \quad (8)$$

where T'_K is the rate coefficient for escape of photons in a radial direction from the near side of annulus KL, and T''_K is the corresponding coefficient for escape in the same direction from the far side of annulus KL; g_{xK} is the radial thickness of the annulus. The expression for I_{out} includes no solid angle factor because with any practical detector there will be a cone of acceptance such that the increasing divergence of the cone will compensate for the decreasing solid angle subtended by the detector as the light source moves further away. In the current version of the computer program values of I_{out} are calculated at three preselected values of L at each time step and stored for subsequent Fourier analysis.

Evaluation of the I, G and T parameters in eqns. (7) and (8) involves making use of the basic theory of resonance absorption and line broadening. The contour of the unreversed line emitted by hot atoms in the source lamp has been calculated by numerical integration of equation (101) of Mitchell and Zemansky [6]:

$$k_\omega = \frac{k_0 \alpha}{\pi} \int_{-\infty}^{\infty} \frac{e^{-y^2}\, dy}{\alpha^2 + (\omega - y)^2} \quad (9)$$

where the peak "Doppler-only" absorption coefficient k_0 is given by:

$$k_0 = \frac{2}{\Delta \nu_D} \left(\frac{\ln 2}{\pi}\right)^{1/2} \frac{\lambda_0^2}{8\pi} (g_2 N / g_1 \tau) \quad (10)$$

and the Doppler width $\Delta \nu_D$ is given by:

$$\Delta \nu_D = 2(2 \ln 2)^{1/2} (RT/M)^{1/2} \nu_0 / c \quad (11)$$

Here ν_0 ($= c/\lambda_0$) is the centre frequency of the line, N is the number of fluorescers of atomic mass M per cm^3, g_1 and g_2 are the degeneracies of the ground and excited states, and τ ($= 1/A$) is the radiative lifetime of the excited state. The parameters ω and α are defined by:

$$\omega = 2(\ln 2)^{1/2} (\nu - \nu_0)/\Delta\nu_D \tag{12}$$

and

$$\alpha = (\ln 2)^{1/2} (\Delta\nu_N + \Delta\nu_L)/\Delta\nu_D \tag{13}$$

The natural linewidth $\Delta\nu_N$ is given by:

$$\Delta\nu_N = 1/2\pi\tau \tag{14}$$

and the Lorentz width $\Delta\nu_L$ by:

$$\Delta\nu_L = Z_L/\pi \tag{15}$$

The frequency of Lorentz-broadening collisions is given by:

$$Z_L = \sigma_L^2 N_L (8\pi RT/\mu)^{1/2} \tag{16}$$

where μ is the reduced mass of the emitter and its collision partner, whose concentration is N_L per cm^3. For most of the present work the Lorentz cross-section σ_L^2 was given a "typical" value of 6×10^{-15} cm^2. For self-broadening by argon the cross-section was taken as 1.14×10^{-14} cm^2, which is the value calculated by using the equation of Weisskopf for Holtzmark broadening, as quoted by Mitchell and Zemansky, at 300 K.

The exciting lamp intensity at a given ω was taken as k_ω multiplied by an arbitrary factor of 10^{12}. The lamp output was allowed to be attenuated by a filter layer having a lower temperature and Doppler width, before entering the fluorescence cell which was assigned a still lower temperature. This is a realistic model of the usual experimental situation[5]. Within the cell at a point a distance z along the axis the absorption rate for the component of frequency specified by ω was calculated as:

$$-\frac{dI_\omega}{dz} = k_\omega I_\omega \exp(-k_\omega z) \tag{17}$$

where I_ω is the intensity of light transmitted by the filter at this frequency. The value of I_{KL} at a point in annulus KL (assumed to be within the exciting beam radius) was obtained by integrating the right hand side of eqn. (17) over $d\nu$, using Simpson's rule and the relation $d\omega = 2(\ln 2)^{1/2} d\nu/\Delta\nu_D$.

To obtain T_k', T_k'' and T_{KL} the rate coefficient for emission of a photon by an excited atom followed by transmission a distance y without being absorbed was calculated, for twenty-five values of y, as the integral

$$T(y) = \frac{2A}{k_0(\pi)^{1/2}} \int_0^\infty k_\omega \, e^{-k_\omega y} \, d\omega \tag{18}$$

This integral was also evaluated using Simpson's rule. For $y = 0$ this typically gave $T = 1.001$ instead of the expected value 1.000. Similarly, the rate coefficient for photon emission and re-absorption after travelling a distance y was calculated as the integral:

$$G(y) = \frac{2A}{k_0(\pi)^{1/2}} \int_0^\infty k_\omega^2 \, e^{-k\omega y} \, d\omega \tag{19}$$

Values of T and G at particular distances required by the problem were then able to be obtained by linear interpolation in tables of G *versus* y^a and T *versus* y^b where $b = a + 1$. The exponent a (typically -1.7) was obtained as the slope of the least squares line in a plot of log G *versus* log y. In this way T'_k and T''_k of eqn. (8) were obtained directly.

The value of T_{KL} was obtained by interpolation as the value of T at $y^b = r^b_{av}$, where r^b_{av} is an average value of r^b, r being the distance from a point on ring KL to the cell wall. Six values of r were obtained as the lengths of vectors directed towards the walls along three perpendicular axes, one axis being parallel to the axis of the fluorescence cell. Eight further values of r^b were obtained from the lengths of vectors directed towards the corners of a cube centred on the point in ring KL and having two of its faces parallel to the end windows of the cell. These eight values of r^b were given a weighting factor of 0.75 when r^b_{av} was calculated.

To calculate r^a_{av} for interpolating in the table of G values four vectors were taken from a point on ring KL to points evenly spaced around ring MN, and the resulting four values of r^a were averaged. This gave a value for the factor $AG(r_{av})$ in eqn. (6). Because of the large number of elements to be calculated for the G_{KLMN} array it was necessary to keep the number of steps involved in determining r_{av} to a minimum. The solid angle factor was approximated by the expression:

$$\Theta_{KLMN}/4\pi = 0.25(g_{zN}\Delta x_{KM} + g_{xM}\Delta z_{LN})x_M/r^3_{av} \tag{20}$$

where x_M is the average radius of annulus MN, g_{zN} is its thickness in the direction of the cell axis, g_{xM} is its radial thickness, Δx_{KM} is the radial distance and Δz_{LN} is the axial distance between rings KL and MN. For the effective thickness R_{KLMN} the smaller of the two values:

$$g_{xM}r_{av}/\Delta x_{KM} \tag{21}$$

or

$$g_{zN}r_{av}/\Delta z_{LN} \tag{22}$$

was used.

The calculations were collected together as a Fortran program which was run on the Oxford University ICL 1906A machine, using 64k of store and taking about four minutes to evaluate the I, G, and T arrays, carry out the integration of eqn. (5) over several hundred time steps, and perform Fourier analyses of the three calculated fluorescence signals.

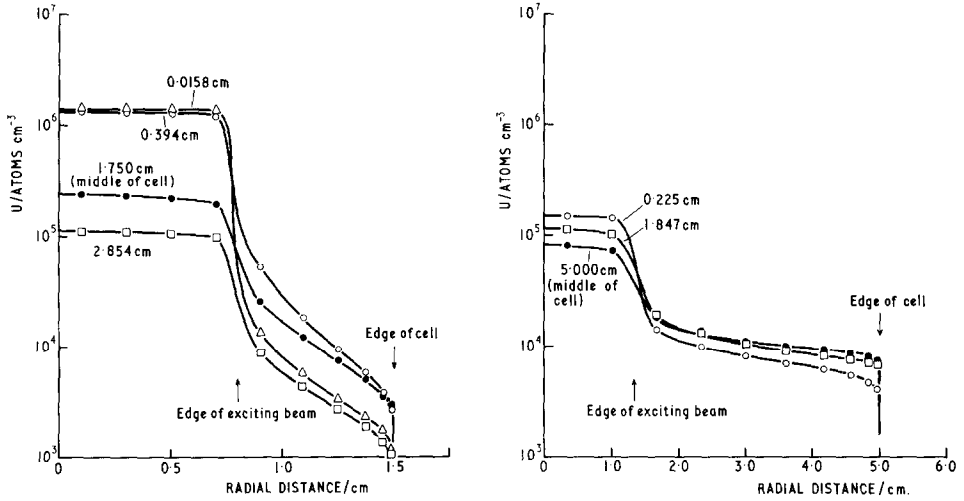

Fig. 1. (a) Representative steady-state concentration profiles for excited cadmium atoms with no quencher present: [Cd] = 2.5 x 10^{14} cm^{-3}; k_0 = 1.171 x 10^3 cm^{-1}. Curves marked with distances from input window. (b) As in (a), for argon: [Ar] = 2.0 x 10^{16} cm^{-3}; k_0 = 1.116 x 10^5 cm^{-1}.

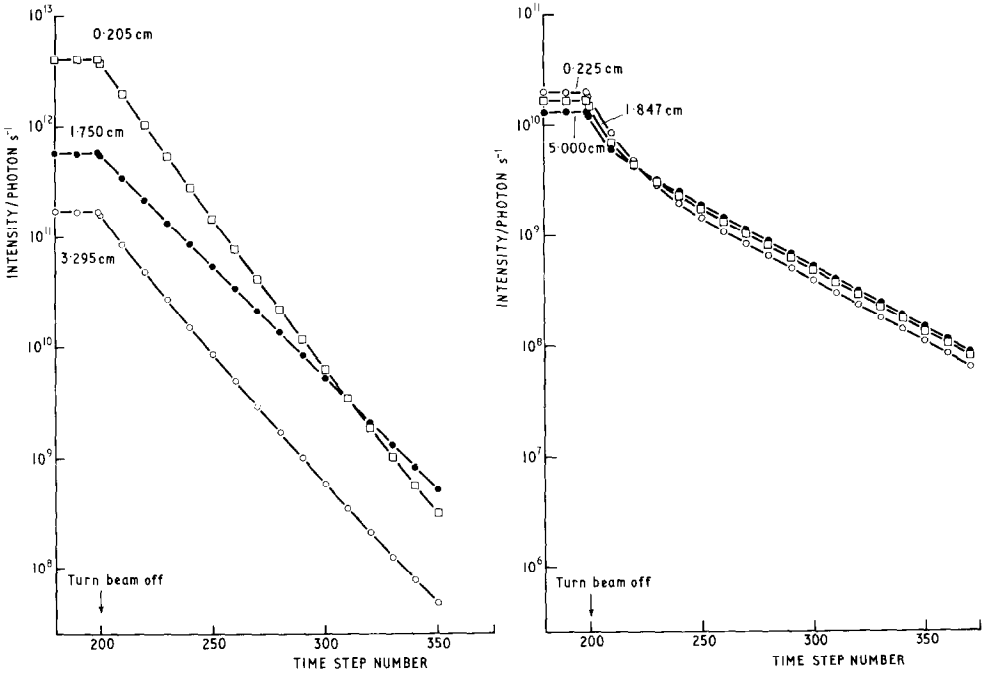

Fig. 2. (a) Decay of Cd 228.8 nm fluorescence with no quencher present. [Cd] = 2.5 x 10^{14} cm^{-3}. Distances from input window marked on curves. Duration of time step = 3 x 10^{-8} s. (b) As in (a) but for argon, [Ar] = 2.0 x 10^{16} cm^{-3}. Duration of time step [= 5 x 10^{-7} s.

Results and Discussion

General form of the results

Some representative concentration profiles for excited species are shown in Fig. 1 and some typical fluorescence decay curves are plotted in Fig. 2. Even when the optical depth is very great it is apparent that the bulk of the excited atom population is located along the path of the exciting beam, and that the greater part of the fluorescence escaping from the cell comes from the region that is illuminated by the incident beam; the region between the beam and the cylinder wall acts mainly as a trapping filter. For the cadmium fluorescence ($k_0 \sim 10^3\ cm^{-1}$) departures from exponential decay are just noticeable when the viewing point is close to the top or bottom end of the cylindrical cell, but are not detectable when the viewing point is at the centre of the cell. For the argon fluorescence ($k_0 \sim 10^5\ cm^{-1}$) an initial fast transient is followed by exponential decay. The trapping times calculated from phase shifts effectively average these fast and slow decays.

Effects of grid size, filter layer depth, time step duration and boundary conditions

Except near the cell boundaries there appears to be very little difference between the results calculated using a 6 × 9 grid (6 radial divisions, 9 axial) and those calculated using a 10 × 15 or larger grid. This point is illustrated in Fig. 3. Therefore the results described here, which were mainly obtained using a 10 × 15 grid, are not expected to suffer from errors owing to there being an insufficient number of grid points.

The effect of filter depth is summarized in Table 1. The results show that varying the filter depth has a marked effect on the steady-state intensity of fluorescence but has very little effect on the trapping time or fluorescence

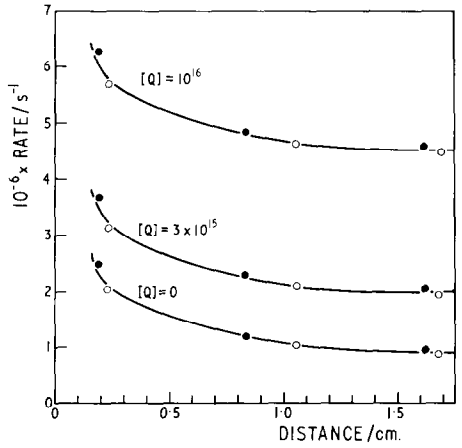

Fig. 3. Dependence of decay rate on distance from the point of entry of the exciting beam. Results calculated with no allowance for losses through the beam exit window. Open circles are points obtained using a 6 × 9 grid; closed circles are values calculated using a 10 × 15 grid. System: Cd 228.8 nm fluorescence quenched by nitrogen.

TABLE 1

Effect of filter thickness. Results for cadmium 228.8 nm radiation partially quenched by N_2. ($Q = 3.6 \times 10^5\ s^{-1}$. Results at three different viewing positions are shown 2.3226(12) = 2.3226×10^{12}. Decay rates derived from calculated phase shifts at fundamental modulation frequency.)

Filter thickness (cm)	Intensity, steady state	Decay rate (s^{-1})
0.05	4.6147 (12)	5.9642 (6)
	8.7401 (11)	2.7192 (6)
	1.6498 (11)	5.7753 (6)
0.50	2.3226 (12)	5.9579 (6)
	7.1524 (11)	2.7268 (6)
	1.5497 (11)	5.7980 (6)
5.00	2.0203 (12)	5.9092 (6)
	2.2490 (11)	2.7365 (6)
	7.1226 (10)	5.8407 (6)

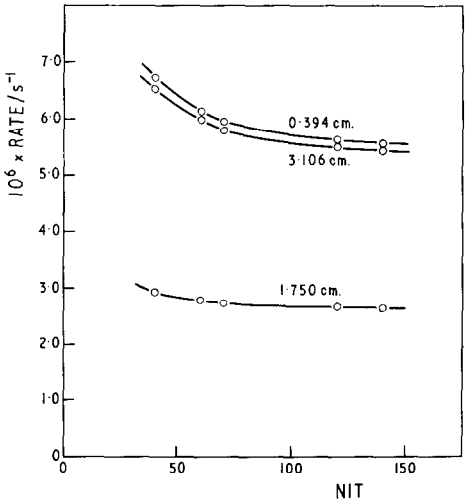

Fig. 4. Dependence of calculated decay rates on NIT, the number of time steps used in reaching the steady state intensity. Data for Cd 228.8 nm fluorescence at different distances from the point of entry of the exciting beam, as shown.

decay rate derived from the phase shift between the exciting light and the fluorescence. In a practical situation this would mean that an alteration of the position of the discharge in a microwave-powered exciting lamp would be likely to have a large effect on the measured intensity of fluorescence but only a slight effect on the phase angle measured at quadrature in the normal way.

The calculated steady-state intensity is not sensitive to the value of NIT, the number of integration steps required to reach the steady state, but the

calculated decay rate is fairly sensitive to this parameter, especially when the number of steps is 60 or less. This is a matter affecting the accuracy of the calculations rather than the behaviour of a practical system. To minimize errors from this source the value of NIT has been kept roughly constant at 100, and when comparisons have been made between results of different calculations any remaining differences in NIT have been compensated for with the aid of curves such as those in Fig. 4.

In many practical situations it is convenient to have a Wood's horn, instead of a window, where the exciting beam leaves the region of interest. This case was simulated approximately by omitting the contribution of the lower window to the loss of photons *via* the term T_{KL}. The results thus obtained were of similar form to those which were obtained with losses from both end windows included, the only significant difference being that the calculated trapping times were uniformly larger, typically by a factor of two or more depending on which part of the cell was being considered.

Comparison of observed and calculated trapping times

Results were obtained for cadmium 228.8 nm radiation with 2.5×10^{14} cadmium atoms per cm^3, for comparison with the results of Morten *et al.* [7] and for argon 106.7 nm radiation at argon pressures near 10^{17} atoms per cm^3, for comparison with the results of Chapman *et al.* [8]. For the cadmium calculations a cell of diameter 3.00 cm and length 3.50 cm was used, with exciting beam diameter 1.60 nm and filter thickness 0.5 cm. For argon a cell of 10 cm length and 10 cm diameter was used, with an exciting beam diameter of 2.667 cm and filter thickness 10.0 cm. These parameters do not agree exactly with those used in refs. 7 and 8. In ref. 7 the fluorescence cell had Wood's horns facing both the entrance and exit directions so that trapping times would be expected to be larger by a factor of about two in comparison with the cell having no Wood's horns (see Fig. 3). In ref. 8 the beam diameter was only 1.0 cm; it appeared preferable to make the calculations for a larger beam so that at least two volume elements could be included in the illuminated volume. The results in Table 2 show that the agreement between observed and calculated trapping times is quite good when it is considered that the experimental systems do not correspond exactly to the theoretical model, and that the trapping times in ref. 8 were obtained by fitting the results to an exponential. The decrease in our calculated trapping times on going from 8×10^{16} to 3×10^{17} argon atoms per cm^3 appears to be associated with the large Holtsmark broadening of the absorption line at the higher argon pressure.

Variation of trapping time and steady-state intensity with quenching rate

The aim here is to determine how well the calculated intensity and decay time of fluorescence obey a Stern–Volmer equation of the form:

$$I_0/I = T_0/T = 1 + k[Q]T_0 \qquad (23)$$

TABLE 2

Comparison of observed and calculated trapping times in the absence of quencher. Values for cadmium refer to mid-point of fluorescence cell. Trapping times T in μs. Natural lifetimes: $\tau = 2 \times 10^{-9}$ s (Cd); $\tau = 8.3 \times 10^{-9}$ s (Ar). T_{calc} derived from phase-shift of fundamental component of fluorescence signal.

Resonance line	Atoms/cm^3	Remarks	T_{obs}	Ref.	T_{calc}
Cd 228.8 nm	2.5×10^{14}	No Wood's horn allowance	0.98 to 1.69	[7]	0.635
Cd 228.8 nm	2.5×10^{14}	One Wood's horn	0.98 to 1.69	[7]	1.05
Ar 106.7 nm	3.0×10^{17}	(a) 0.225 cm from window	8.0	[8]	8.78
		(b) 1.847 cm from window			12.30
		(c) 5.000 cm from window			26.04
Ar 106.7 nm	8.0×10^{16}	(a)	5.0	[8]	10.44
		(b)			13.05
		(c)			17.70
Ar 106.7 nm	2.0×10^{16}	(a)	2.0	[8]	7.65
		(b)			8.49
		(c)			9.69
Ar 106.7 nm	5.0×10^{15}	(a)	—		5.22
		(b)			5.37
		(c)			5.67

Equation (23), for trapping times T rather than intensities I, was used in ref. 7 to evaluate rate constants for quenching of Cd 228.8 nm fluorescence. Theoretical results are given in Table 3 for quenching by nitrogen, for which the quenching rate constant given in reference 7 is 3.6×10^{-10} cm^3 molecule^{-1} s^{-1}. Values of I_0/I are given both for the steady-state intensity and for the amplitude of the fundamental component as obtained by Fourier analysis of the output signals. The two I_0/I values are always very similar, as is to be expected since the fundamental component is much the greatest constituent (~95%) of the fluorescence waveform.

The main conclusion to be drawn from Table 3 is that with experimentally measured trapping times a plot of T_0/T *versus* [Q] should give k_Q values of quite acceptable accuracy. The agreement with the Stern–Volmer predictions is improved if $1/T$ is plotted against [Q] instead of T_0/T, since the T_0/T values in Table 3 are systematically too high by a few percent. The agreement of the I_0/I values with those predicted from the Stern–Volmer equation is also good except at points close to the point of entry of the exciting beam.

TABLE 3

Calculated I_0/I and T_0/T values for Cd 228.8 nm radiation, at positions 0.205 cm, 1.750 cm and 2.295 cm from the point of entry of the exciting beam (cell length 3.50 cm). The last column contains the values predicted by eqn. (23) for Q = N_2 and $k_Q = 3.6 \times 10^{-10}$ cm^3 molecule^{-1} s^{-1}, with T_0 values of 0.4418, 0.6347 and 0.4860 μs, at the three viewing positions.

Q/cm^3	I_0/I (amplitude)	I_0/I (steady state)	T_0/T	$1 + k_Q[Q]T_0$
1.0×10^{15}	1.169	1.163	1.166	1.159
	1.246	1.173	1.233	1.229
	1.190	1.184	1.187	1.175
3.0×10^{15}	1.501	1.484	1.498	1.478
	1.740	1.721	1.706	1.686
	1.568	1.551	1.561	1.524
1.0×10^{16}	2.600	2.553	2.663	2.592
	3.439	3.395	3.366	3.285
	2.864	2.818	2.850	2.748
3.0×10^{16}	5.366	5.514	6.001	5.777
	8.260	8.092	8.126	7.855
	6.552	6.748	6.512	6.243
6.0×10^{16}	8.540	8.490	11.12	10.56
	14.99	14.28	15.42	14.71
	11.77	11.74	12.12	11.49
1.0×10^{17}	12.16	11.94	17.72	16.92
	24.31	24.18	24.85	23.85
	19.12	18.84	19.35	18.48

Acknowledgements

The author is grateful to the Oxford University Computer Laboratory for the generous provision of facilities and advice, to Dr. R. P. Wayne for helpful discussions, and to Professor J. S. Rowlinson for the hospitality of his Department.

References

1 L. F. Phillips, J. Photochem., 2 (1973) 255.
2 T. Holstein, Phys. Rev., 72 (1947) 1212.
3 P. Walsh, Phys. Rev., 116 (1959) 511.
4 C. von Trigt, Phys. Rev., 181 (1969) 97.
5 G. Van Volkenburgh and T. Carrington, J. Quant. Spectros. Radiat. Transfer, 11 (1971) 1181.
6 A. C. G. Mitchell and M. W. Zemansky, Resonance Radiation and Excited Atoms, Cambridge University Press, Cambridge, 1934.
7 P. D. Morten, C. G. Freeman, R. F. C. Claridge and L. F. Phillips, J. Photochem., 3 (1974) 285.
8 M. J. Boxall, C. J. Chapman and R. P. Wayne, J. Photochem., 4 (1975) 281.